

See discussions, stats, and author profiles for this publication at: <https://www.researchgate.net/publication/248515607>

# Relationships between the kinematics of the top of a layer and the state of stress within it due to block motion at ....

Article in *Journal of Geodynamics* · December 1988

DOI: 10.1016/0264-3707(88)90019-1

CITATIONS

8

READS

11

5 authors, including:



Yu. L. Rebetsky

Russian Academy of Sciences

197 PUBLICATIONS 587 CITATIONS

[SEE PROFILE](#)

Some of the authors of this publication are also working on these related projects:



Tectonophysical data on natural stress in the field of hydraulic fracturing of gas producing formation  
[View project](#)



5-Books of colleagues [View project](#)

**RELATIONSHIPS BETWEEN THE KINEAMATICS OF THE TOP OF  
A LAYER AND THE STATE OF STRESS WITHIN IT DUE TO  
BLOCK MOTION AT ITS BOTTOM**  
(in connection with the interpretation of recent movements)

A. S. GRIGORYEV, I. M. VOLOVICH, A. V. MIKHAILOVA,  
YU. L. REBETSKY and Z. E. SHAKHMURADOVA

*Institute of Physics of the Earth, USSR Acad. Sci., Moscow, U.S.S.R.*

(Accepted August 5, 1988)

**ABSTRACT**

Grigoryev, A. S., Volovich, I. M., Mikhailova, A. V., Rebetsky, Yu. L. and Shakhmuradova, Z. E., 1988. Relationships between the kinematics of the top of a layer and the state of stress within it due to block motion at its bottom (in connection with the interpretation of recent movements). *In*: Yu. D. Boulanger, S. Holdahl and P. Vyskočil (Editors), *Recent Crustal Movements. Journal of Geodynamics*, 10: 127-138.

The equilibrium of an infinite linearly viscous layer overlying a rigid basement which is separated into blocks by a narrow plane slit is considered. The state of stress in the layer is caused by slow translational motions of the basement blocks. This spatial problem is shown to separate into problems of plane and anti-plane strain; their solutions are constructed in analytic form. The theoretical study was accompanied by modelling experiments. The results are applied to a kinematic interpretation of recent movements in sediments.

Consider an infinite horizontal layer of constant thickness consisting of a linearly viscous material which overlies a rigid half-space divided by a narrow plane slit into two semi-infinite blocks. We assume complete or partial cohesion between the layer and the basement. Our goal is to determine the state of stress and velocity of displacement due to translation of the basement blocks relative to one another occurring parallel to the middle plane of the slit. The motion is assumed to be so slow that the state of the layer can be regarded as being in equilibrium. The time under consideration is restricted to such an interval that the displacements of the layer are small compared with its thickness. We assume the original plane of contact between the layer and the basement to be a fixed set of coordinates, the  $z$ -axis pointing along the middle slit plane (see Fig. 1). Let  $\beta$  denote the angle between the vertical plane and the middle plane, varying within the range  $-(\pi/2 < \beta < (\pi/2))$ .

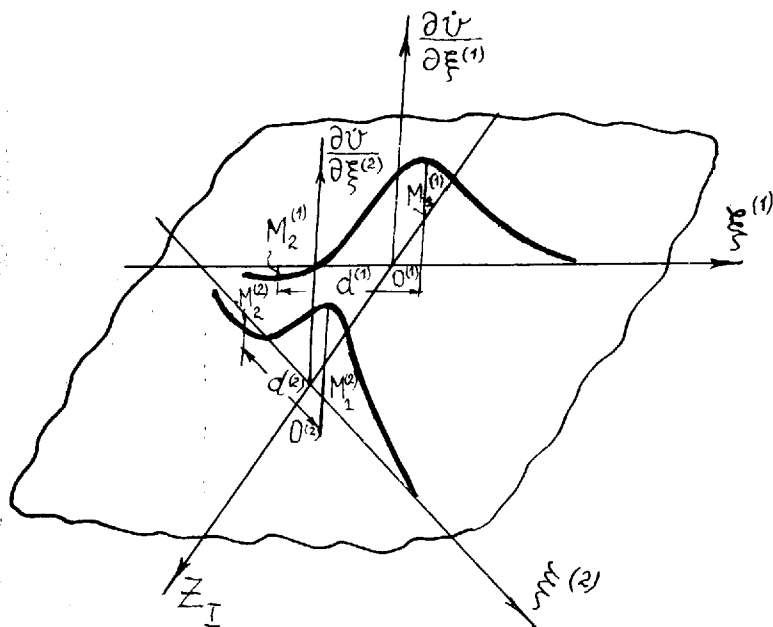


Fig. 5. Determination of the position of the  $z_1$ -axis from the derivatives of vertical velocity along two arbitrarily chosen directions  $\xi^{(1)}$  and  $\xi^{(2)}$ .

Having found the fault position and orientation, one can determine  $\dot{V}_0$  and  $\dot{W}_0$  from formulae requiring the values of "measured" rates  $\tilde{V}$  and  $\tilde{W}$  only, such as

$$\dot{V}_0 = 1,21H \left( \frac{\partial \tilde{V}}{\partial x} \right)_{x=0}; \quad \dot{W}_0 = 2H \left( \frac{\partial \tilde{W}}{\partial x} \right)_{x=0}, \quad \text{or} \quad (15)$$

$$\dot{V}_0 = 1,48[\tilde{V}(0,5H) - \tilde{V}(-0,5H)]; \quad \dot{W}_0 = 2,2[\tilde{W}(0,5H) - \tilde{W}(-0,5H)]; \quad (16)$$

$$\dot{V}_0 = 1,11[\tilde{V}(H) - \tilde{V}(-H)]; \quad \dot{W}_0 = 1,35[\tilde{W}(H) - \tilde{W}(-H)].$$

For the case a single fault at distances that exceed approximately  $2H$  to the right and left of the  $z_1$ -axis, the surface velocity components, let us label them  $\dot{U}_{\text{right}}$  and  $\dot{U}_{\text{left}}$ ,  $\dot{V}_{\text{right}}$  and  $\dot{V}_{\text{left}}$ ,  $\dot{W}_{\text{right}}$  and  $\dot{W}_{\text{left}}$ , can be considered equal to the bottom velocity, which leads to

$$\dot{U}_0 = \tilde{U}_{\text{right}} - \tilde{U}_{\text{left}}; \quad \dot{V}_0 = \tilde{V}_{\text{right}} - \tilde{V}_{\text{left}}; \quad \dot{W}_0 = \tilde{W}_{\text{right}} - \tilde{W}_{\text{left}}. \quad (17)$$

Formulas (14)–(17), as well as information on  $\dot{u}(x)$ , can be used as a check on the results. In cases in which "basic" geologic and geophysical informa-

tion for a region provides enough evidence to consider the basement of the sedimentary cover as a system of several blocks separated by active faults, one can directly apply the above technique of data analysis, provided the mutual effect of adjacent faults on the surface kinematics can be disregarded. Each fault can be considered as a "single" one, if there are distances of the order  $4H$  or more between adjacent faults. We shall only need a unified choice of the constant  $V_*$  and the connection of all data to a unified system of coordinates during the final determination of the kinematics of basement blocks.

In natural conditions, one encounters active faults that are spaced at intervals of the order of  $H$  to  $2H$ , and the problem of interpretation becomes much more complicated. It is important to point out, however, that the first stage should again involve only data on vertical velocities of the surface, and one should begin by plotting  $\tilde{V}(\xi)$  and  $\partial\tilde{V}/\partial\xi$  and analysing these curves. Zones of closely spaced faults will show in these curves as stationary points with no intervening segments within which  $\tilde{V}(\xi) = \text{const}$ . A method of successive approximations may be suggested to determine fault position and orientation in such zones. Calculations (see Grigoryev *et al.* (1979b)) for the cases of a three-block basement as well as for the cases in which the angle between fault plane and the vertical plane does not exceed  $10-15^\circ$ , have shown that the stationary point with ordinate  $M_1$  on the curve  $\partial\tilde{v}/\partial x$  lies directly above the fault, even with closely spaced faults. As a first approximation, one can thus assume that an active basement fault corresponds to each stationary point in the plot of  $\partial\tilde{V}/\partial\xi$ , and determine the position and direction of the intersections of the faults with the layer bottom. Further, one should turn to the analysis of the character of curves  $\tilde{V}(x)$  and  $\partial\tilde{V}/\partial x$  along segments containing two adjacent stationary points. One should make use of the method of superposition of solutions to construct a theoretical solution for each segment and then join them onto one another, arriving at theoretical results that describe the movements of the surface and the layer bottom in the region as a whole. A full kinematic picture of basement block motion will be found when one adds information on the velocity of block motion "along" the faults, that is,  $\dot{W}(x)$  data, in the case that this is available. It should be pointed out, however, that the spatial problem requires referring  $\dot{W}(x)$ , as well as  $\tilde{V}(x)$  and  $\dot{U}(x)$  to a single origin.

In addition to theoretical investigations, modelling experiments have been carried out in which we studied the kinematics of the layer surface, the strain field within the layer, and the initiation and development of fractures. A joint analysis of the results has revealed some persistent characteristics of deformation that can have prognostic value: the correlation between isolines of stress and strain, the occurrence of fractures in theoretical zones of increased stress etc. Data on the gradients of vertical velocities observed at

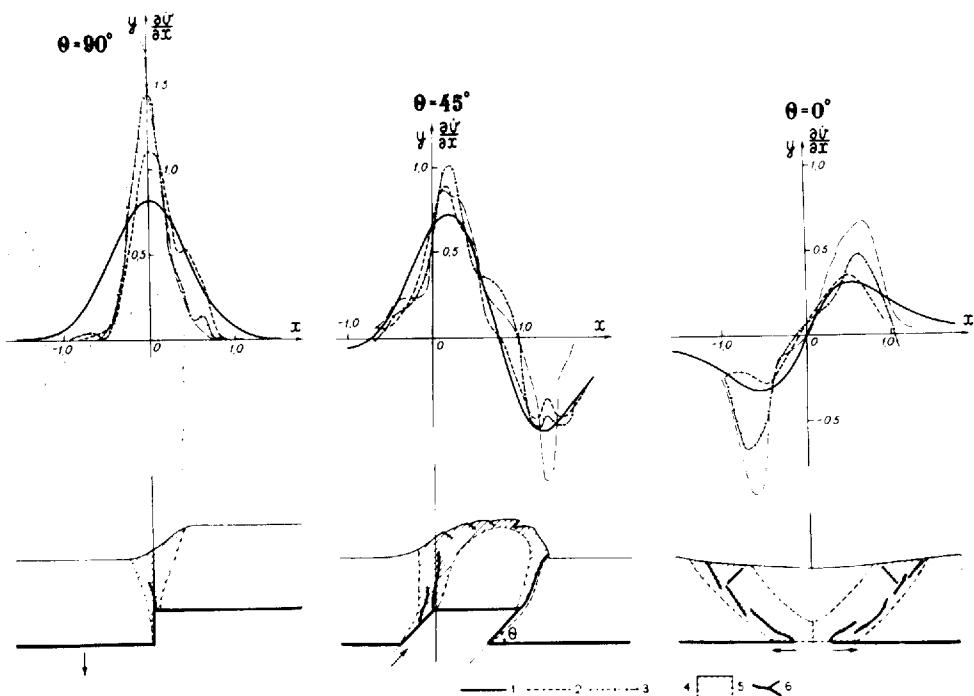


Fig. 6. Relation of vertical surface velocity gradient in superfault zones to fracture regions in the layer and to the orientation of the fault itself. (1) theoretical gradient curve for the initial stage, (2) the gradient curve for the initial stage as found from experimental data, (3, 4) the same for subsequent stage, (5) crack zone, (6) large fractures in the layer.

the surface of a layer in experiments for the three cases of deformation shown in Fig. 6 are in satisfactory agreement with the theoretical results. This provides additional corroboration for the use of theoretical relationships that have formed the basis of the above technique for the kinematic interpretation of recent movements.

## REFERENCES

- Grigoryev A. S., Mikhailova A. V. and Shakhmuradova Z. E., 1979a. Relationship between the characteristics of vertical surface displacements and the state of stress in the sedimentary cover within superfault zones. *In: Stress and Strain Fields in the Lithosphere*. Nauka, Moscow, p. 97-125 (in Russian).
- Grigoryev A. S., Mikhailova A. V. and Shakhmuradova Z. E., 1979b. On kinematic characteristics of the motion of the diurnal surface and the stress state of the sedimentary cover in zones above basement faults. *Izv. AN SSSR, Fizika Zemli (Solid Earth)*, No. 1, p. 3-20 (in Russian).
- Grigoryev A. S. and Mikhailova A. V., 1985. Combining theoretical and experimental methods to investigate the creation of tectonic features. *In: Experimental Tectonics in Theoretical and Applied Geology*. Nauka, Moscow, p.131-146. (in Russian).

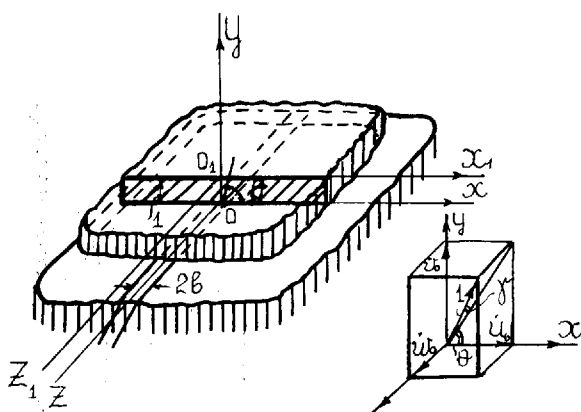


Fig. 1. Statement of the problem illustrated.

From the formulation of the problem it follows that the components of the stress tensor and of the displacement velocity vector at any point within the layer will not depend on  $z$ , even though the problem is in three dimensions as ordinarily understood. The original set of equations separates into two sets. We write them down in dimensionless variables, assuming a massless layer

$$\frac{\partial p_x}{\partial x} + \frac{\partial p_{xy}}{\partial y} = 0, \quad \frac{\partial p_{xy}}{\partial x} + \frac{\partial p_y}{\partial y} = 0, \quad p_x - \frac{1}{2}(p_y + p_z) = \frac{3}{4} \frac{\partial u}{\partial x}, \quad (1)$$

$$p_y - \frac{1}{2}(p_z + p_x) = \frac{3}{4} \frac{\partial v}{\partial y}, \quad p_z - \frac{1}{2}(p_x + p_y) = 0, \quad p_{xy} = \frac{1}{4} \left( \frac{\partial u}{\partial y} + \frac{\partial v}{\partial x} \right),$$

$$\frac{\partial p_{zx}}{\partial x} + \frac{\partial p_{yz}}{\partial y} = 0, \quad p_{zx} = \frac{1}{4} \frac{\partial w}{\partial x}, \quad p_{yz} = \frac{1}{4} \frac{\partial w}{\partial y}. \quad (2)$$

Here  $x$ ,  $y$ ,  $z$  are the coordinates divided by  $H$ , the layer thickness;  $p_x$ ,  $p_y$ ,  $p_z$ ,  $p_{xy}$ ,  $p_{zx}$  are stresses divided by  $4\eta V_*/H$  where  $\eta$  is the viscosity,  $V_*$  is a constant having the dimension of velocity;  $u$ ,  $v$ ,  $w$  are the velocities  $\dot{U}$ ,  $\dot{V}$ ,  $\dot{W}$  in the  $x$ ,  $y$ ,  $z$  directions divided by  $V_*$ . The set (1) is the resolving one in the problem of plane strain for an incompressible linearly viscous body, and can, after introducing the stress function  $\varphi$ , be reduced (see, for example, Grigoryev *et. al.* (1979a), Grigoryev *et. al.* (1979b)) to a biharmonic equation

$$\nabla^4 \varphi = 0. \quad (3)$$

The set (2) is the resolving one for the problem of antiplane strain and can be reduced to a harmonic equation

$$\nabla^2 \dot{w} = 0. \quad (4)$$

The boundary conditions correspond to no stress at the top of the layer, while at the bottom we have the fixed conditions of contact between the bottom of the layer and the basement. Since we must have the possibility of motion at the bottom, these conditions are conveniently written in the rate of displacement, even though this is quite formal.

The boundary conditions can also be separated into two sets

$$y = 1: p_y = p_{xy} = 0, \quad y = 0: \dot{u} = \omega(x), \quad \dot{v} = \psi(x), \quad (5)$$

$$y = 1: p_{yz} = 0, \quad y = 0: \dot{w} = \zeta(x). \quad (6)$$

Combining (5) and the system (1) will give a biharmonic boundary value problem for an infinite strip  $0 \leq y \leq 1$ ,  $z = 0$ , while combining (6) and system (2) will give a harmonic one. The boundary conditions in both problems are mixed. The solution of the above problem is obtained by superposing the solutions of (3) under the conditions (5) upon those of (4) under the conditions (6). Then one has to add the solution of the problem of equilibrium for the layer under the action of its own weight alone; the basement blocks are to be regarded as fixed. If there are mixed boundary conditions proper at some finite areas of the bottom or they are assigned in stresses, the method of solution as outlined below can be retained, except that integral equation techniques will have to be used in order to switch to conditions in the rate of displacement.

We now consider one of the possible versions in the formulation of the problem, assuming a wedged contact between the bottom and the basement blocks and some material filling the suture between the two whose properties resemble those of the layer material. If the suture width divided by the layer thickness,  $2b$ , satisfies  $2b \ll 1$ , then  $\omega(x)$ ,  $\psi(x)$  and  $\zeta(x)$  in the range  $|x| \leq 2b$  can be obtained by retaining only linear terms in their expansions in the vicinity of the coordinate origin and making use of continuity in the rate of displacement at the end points of the range. The conditions (5) and (6) will then be

$$y = 0: \omega(x) = \frac{\dot{u}_0}{2b} x; \quad \psi(x) = \frac{\dot{v}_0}{2b} x \quad \text{for } |x| \leq b, \quad \omega(x) = \frac{\dot{u}_0}{2} \text{sign } x, \quad (7)$$

$$\psi(x) = \frac{\dot{v}_0}{2} \text{sign } x \quad \text{for } |x| \geq b;$$

$$y = 0: \zeta(x) = \frac{\dot{w}_0}{2b} x \quad \text{for } |x| \leq b, \quad \zeta(x) = \frac{\dot{w}_0}{2} \text{sign } x \quad \text{for } |x| \geq b. \quad (8)$$

Here  $\dot{u}_0$ ,  $\dot{v}_0$ ,  $\dot{w}_0$  are the projections of a dimensionless  $\dot{S}_0$  on the coordinate axes, where  $\dot{S}_0$  is the rate of relative motion of the blocks, the right one relative to the left. If  $V_* = |\dot{S}_0|$  then (see Fig. 1)

$$\dot{u}_0 = \cos \theta \cos \gamma, \quad \dot{v}_0 = \sin \theta \cos \gamma, \quad \dot{w}_0 = \sin \gamma. \quad (9)$$

Under the above assumptions, the problem of equilibrium for a layer under its own weight can be written in the form

$$p_x = p_y = p_z = -K_1(1-y); \quad p_{xy} = p_{yz} = p_{zx} = \dot{u} = \dot{v} = \dot{w} = 0; \quad K_1 = \frac{\varphi g H^2}{4\eta V}, \quad (10)$$

where  $\varphi$  is the density of the material and  $g$ —the acceleration due to gravity.

The solution of (3) under the conditions (7), based on a Fourier integral representation of the stress function, will yield the desired formulæ for stresses and the rate of displacement entering (1); the remaining functions are to be determined from the solution of equation (4) under the boundary conditions (8). This solution is constructed similarly to the preceding ones, based on a Fourier intergral representation of  $\dot{w}$ . Superposing the solutions, we obtain as a final result

$$p_x = \frac{\cos \gamma}{2\pi} \left\{ \sin \theta \int_0^\infty \varphi_{11}(\alpha, y) T(\alpha) \sin \alpha x \, d\alpha - \cos \theta \int_0^\infty \varphi_{12}(\alpha, y) T(\alpha) \cos \alpha x \, d\alpha \right\} - K(1-y), \quad (11)$$

$$p_y = \frac{\cos \gamma}{2\pi} \left\{ \sin \theta \int_0^\infty \varphi_{21}(\alpha, y) T(\alpha) \sin \alpha x \, d\alpha - \cos \theta \int_0^\infty \varphi_{22}(\alpha, y) T(\alpha) \cos \alpha x \, d\alpha \right\} - K_1(1-y),$$

$$p_z = \frac{1}{2}(p_x + p_y),$$

$$p_{xy} = \frac{\cos \gamma}{2\pi} \left\{ -\sin \theta \int_0^\infty \varphi_{31}(\alpha, y) T(\alpha) \cos \alpha x \, d\alpha + \cos \theta \int_0^\infty \varphi_{32}(\alpha, y) T(\alpha) \sin \alpha x \, d\alpha \right\},$$

$$p_{yz} = -\frac{\sin \gamma}{8\pi b} \ln \frac{\left[ \cosh(\pi/2)(x-b) + \cos(\pi/2)y \right] \times \left[ \cosh(\pi/2)(x+b) - \cos(\pi/2)y \right]}{\left[ \cosh(\pi/2)(x-b) - \cos(\pi/2)y \right] \times \left[ \cosh(\pi/2)(x+b) + \cos(\pi/2)y \right]}$$



$$p_{zx} = \frac{\sin \gamma}{8\pi b} \left[ \tan^{-1} \frac{\sinh(\pi/2)(x+1)}{\sin(\pi y/2)} - \tan^{-1} \frac{\sinh(\pi/2)(x-b)}{\sin(\pi y/2)} \right],$$

$$\dot{u} = \frac{\cos \gamma}{\pi} \left\{ -\sin \theta \int_0^\infty \varphi_{41}(\alpha, y) \frac{T(\alpha)}{\alpha} \cos \alpha x \, d\alpha \right. \\ \left. + \cos \theta \int_0^\infty \varphi_{42}(\alpha, y) \frac{T(\alpha)}{\alpha} \sin \alpha x \, d\alpha \right\},$$

$$\dot{v} = \frac{\cos \gamma}{\pi} \left\{ \sin \theta \int_0^\infty \varphi_{51}(\alpha, y) \frac{T(\alpha)}{\alpha} \sin \alpha x \, d\alpha \right. \\ \left. - \cos \theta \int_0^\infty \varphi_{52}(\alpha, y) \frac{T(\alpha)}{\alpha} \cos \alpha x \, d\alpha \right\},$$

$$\dot{w} = \frac{\sin \gamma}{\pi} \int_0^\infty \frac{\cosh \alpha(1-y)T(\alpha)}{\cosh \alpha} \sin \alpha x \, d\alpha.$$

Here  $T(\alpha) = \sin \alpha b / \alpha b$ ; when  $b \rightarrow 0$ ,  $T(\alpha) \rightarrow 1$ ;  $\varphi_{ki}(\alpha, y)$  ( $k = 1, 2, 3, 4, 5$ ;  $i = 1, 2$ ) are functions that were found when solving (3) under the specification of the boundary conditions (5) in the form (7); the expressions for these functions can be found in Grigoryev *et. al.* (1979a) and Grigoryev *et. al.* (1979b). It should be noted that, since the method of "superposition" is applicable, the solution yields ready-made results also for the case of a multiblock basement, provided the traces of the fault planes at the layer bottom are parallel to one another. The isolines of greatest tangential stress and "equivalent" (in the sense of Mohr) stresses were obtained by means of a numerical realization of the solutions for plane strain and longitudinal shear. This has allowed us to show that the typical pattern of stress state for each  $\theta$  is confined to a superfault zone, and to identify zones of increased stress within the layer. There is a significant concentration of stress around the fault suture; when one moves towards the points  $y = 0$ ,  $x = b$  the stresses increase indefinitely, but the relevant singularities at  $b \neq 0$  are integrable, and the forces applied to the layer bottom can be calculated. If  $b \leq 0.01$ , the results of the asymptotic solution ( $b = 0$ ) can be used for determining stresses within the layer everywhere, except for a very small vicinity of singular points; the same applies to the kinematics of the free surface of the layer. A study of this has revealed characteristic features relating the curves of the velocity and its gradient at the surface to the position and orientation of the slit that separates the basement blocks, as well to their relative rate of motion.

We now briefly discuss the kinematics of the free surface of the layer. We define an additional set of coordinates  $x_1, 0, z_1$  (see Fig. 1); obviously  $x_1 = x$  and  $z_1 = z$ .

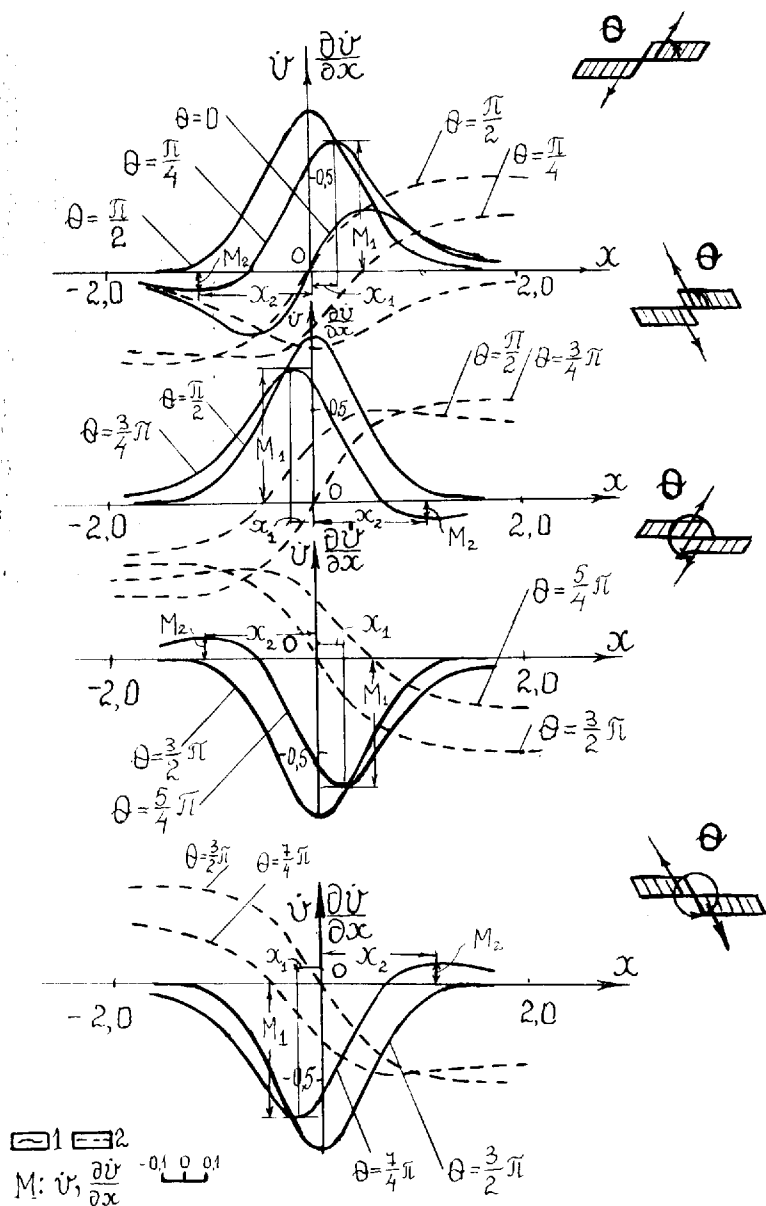


Fig. 2. Dimensionless vertical velocity and its gradient at the free surface of a layer for various (shown on the right) fault orientations and relative velocity directions of basement blocks. (1) —  $\partial \dot{v} / \partial x$ -gradient, (2)  $\dot{v}(x)$ -velocity.

Fig. 2 shows curves which demonstrate the typical behaviour of the vertical velocity and its the derivative with respect to  $x$  at the layer surface for three variants of fault orientation within the whole range, where the direction of relative block motion can vary, at  $\gamma \neq \pi/2$  (see Fig. 1). We shall not describe them in detail, because the corresponding results are partly published in Grigoryev *et. al.* (1985). There are two stationary points of the curves  $\partial\dot{v}/\partial x$  — a maximum and a minimum, lying on the opposite sides of the  $z$ -axis in the general case of the motion along a single inclined fault. If the fault is vertical, there is only one extremum at  $x = 0$ . When the blocks are moving apart in horizontal direction ( $\beta = \pi/2$ ), the ordinates of stationary points are equal in absolute value, and the inflection point of  $\partial\dot{v}(x)/\partial x$  occurs at  $x = 0$ . The curves of the horizontal velocities parallel to the  $z$ -axis,  $\dot{w}(x)$  and  $\partial\dot{w}(x)/\partial x$ , each have one characteristic point — an inflexion in  $\dot{w}(x)$  and an extremum in  $\partial\dot{w}/\partial x$  occur at  $x = 0$ . We note in parentheses that we put  $V_* = \dot{S}_0 |\cos \gamma|$  when passing to the dimensionless velocities  $\dot{v}(x)$  and  $V_* = \dot{S}_0 |\sin \gamma|$  when passing to the dimensionless  $\dot{w}(x)$ . An analysis of a family of curves similar to those given in Fig. 2, has allowed us to construct a diagram showing the relationships (see Fig. 4) between  $\beta$  and the quantities

$$m = \frac{|M_2|}{M_1}, \quad \tilde{x}_1 = \frac{x_1}{d}. \quad (12)$$

Here  $d$  is the distance between the projections of the stationary points on the  $x$ -axis; obviously,  $d = |x_1| + |x_2|$ ;  $x_1$  and  $x_2$  are the abscissas;  $M_1$  and  $M_2$  are the ordinates of the stationary points occurring in the curves  $\partial\dot{v}/\partial x$  (see Fig. 2),  $M_1$  being the greater of the two in absolute value. One can determine  $\beta$  and then  $\tilde{x}_1$  from known values of  $m$  and  $\text{sign } \tilde{x}_1$ , that is, find the origin on the  $x$ -axis. The quantity  $\theta$  is found from

$$\theta = \frac{\pi}{2} - \beta \quad \text{when } m > 0; \quad \theta = \frac{3}{2}\pi - \beta \quad \text{when } m < 0. \quad (13)$$

The results discussed above are useful in the kinematic interpretation of recent movements at the diurnal surface in platform areas with moderate relief at the bottom and the surface, provided the geological and geophysical information on a specific region is sufficient to enable one to make statements as to the thickness of the sedimentary cover and to regard its recent movements as being due to the motion of basement blocks along the intervening faults, and to consider the traces of these latter at the layer bottom to be close to parallel. When we have sufficiently representative evidence relating to the kinematics of the diurnal surface, an analysis of the experimental data will determine more precisely the position and orienta-

tion of previously identified active basement faults, it also will identify hidden ones, as well as determining the rate of relative block motion. We shall consider the solution of such an "inverse" problem first in the simplest case in which nature and the above model are supposed to be correspondence, there being a single active basement fault. It is essential for constructing techniques useful in the interpretation of surface movements that the character of the curves in Fig. 2 and 3 persists when we pass from the argument  $x$  to the argument  $\xi$ , which is also measured from the  $z_1$ -axis along some straight line  $\xi$ . The functions  $\dot{v}(\xi)$  and  $\dot{v}(x)$ ,  $\dot{w}(\xi)$  and  $\dot{w}(x)$  and their derivatives must be different in scale only and the ratios of both abscissas and ordinates of the characteristic points will not depend on the direction of  $\xi$ . This means that the angle  $\beta$  and the position of the  $z_1$ -axis can be determined from the diagram of Fig. 4, together with the plots of  $\partial\dot{v}/\partial\xi$ . The only thing we need to do is to adopt the convention that  $M_1$  and  $M_2$  will be the ordinates of extrema in the curve  $\partial\dot{v}/\partial\xi$  and also that  $\tilde{x}_1 = \tilde{\xi}_1 = \xi_1/d$ , where  $d = |\xi_1| + |\xi_2|$  is the distance between the projections of stationary points on to the  $\xi$ -axis,  $\xi_1$  and  $\xi_2$  being the abscissas of these points. The above statement remains valid irrespective of whether the velocities and coordinates are dimensional or dimensionless.

Solution of the interpretation problem should begin by determining the fault position. This, as well as its orientation, can in the general case be formally obtained from information on the vertical velocity of the surface collected under natural conditions; we shall call these velocities "measured" ones and mark them with a tilde above the letter. A known field of the velocities should be used to plot vertical velocities  $\tilde{V}(\xi)$  and their derivatives  $\partial\tilde{V}/\partial\xi$  along some two straight lines at the surface, that pass in an arbitrary direction  $\xi$ ; it is advisable to deal just with these curves, because they are not dependent on the velocity origin. If a "single" fault is available in a

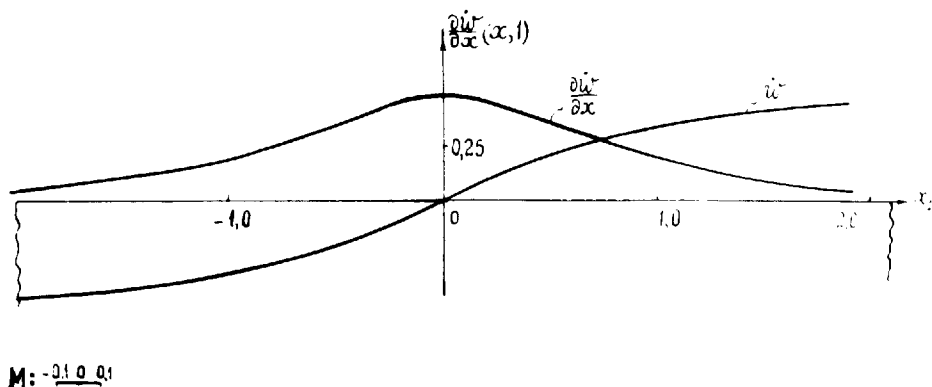


Fig. 3. Theoretical relationships of  $m$  and  $x_1$  plotted against fault orientation.

given region, the plots of  $\partial\tilde{V}/\partial\xi$  must have two stationary points, and the  $z_1$ -axis must intersect the straight lines  $\xi$  between the projections of these points on  $\xi$  (see Fig. 5). Setting the origin of  $\xi$  at the desired point of intersection, one should find  $M_1, M_2, d$ , and sign  $\xi_1$ , and determine  $\beta$  and  $\xi_1$  from the diagram of Fig. 4. One then determines the point of intersection between the lines  $\xi$  and the  $z_1$ -axis;  $\theta$  is found from (13). Then the directions  $x_1$  and  $z_1$  are to be found, hence the direction in which  $\theta$  is measured. If the plots of  $\partial\tilde{V}/\partial\xi$  have only a single stationary point, then the  $z_1$ -axis is the straight line passing through the projections of these points. We shall then have  $m = x_1 = 0$ , the fault plane is vertical. If the vertical velocity should prove to be constant along  $\xi$ , this would mean that the direction  $\xi$  coincides with  $z_1$ , the position of the  $z_1$ -axis, and the angles  $\beta$  and  $\theta$  are determined with the help of  $\partial\tilde{V}/\partial x$  curves, the diagram of Fig. 4 and formulae (13). If vertical velocities should turn out to be zero along any direction, then we have longitudinal shear:  $\dot{U}_0 = \dot{V}_0 = 0, \dot{S}_0 = \dot{W}_0$ . Determination of fault position requires information on horizontal velocities along straight lines passing in an arbitrary directions  $\xi^{(1)}$  and  $\xi^{(2)}$ . One should plot  $\partial\tilde{w}/\partial\xi^{(1)}$  and  $\partial\tilde{w}/\partial\xi^{(2)}$ . Each of these curves, in accordance with the plot in Fig. 4, will have a single stationary point, and the  $z_1$ -axis will be determined as a line passing through the projections of these stationary points. The orientation of the fault plane remains indeterminate in that case, as well as for a separation fault and a combination of longitudinal shear with a separation fault. The  $\dot{S}_0$  vector can be determined from

$$\dot{S}_0 = \sqrt{\dot{U}_0^2 + \dot{V}_0^2 + \dot{W}_0^2}; \quad \text{tg } \gamma = \frac{\dot{W}_0}{\sqrt{\dot{U}_0^2 + \dot{V}_0^2}}; \quad \text{tg } \theta = \frac{\dot{V}_0}{\dot{U}_0}. \quad (14)$$

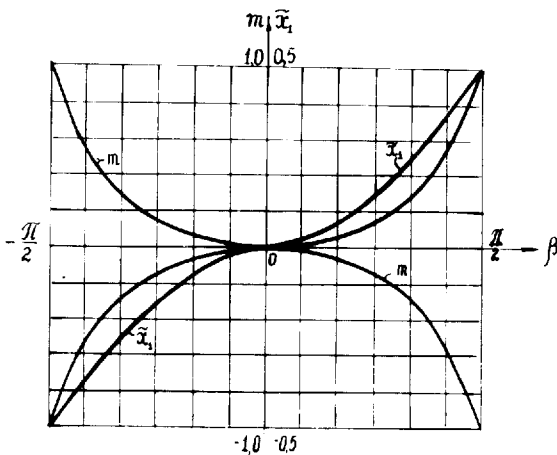


Fig. 4. Horizontal component of the velocity at the free surface corresponding to longitudinal shear, and its gradient  $\partial\tilde{w}/\partial x$ .